



ELSEVIER

Earth and Planetary Science Letters 191 (2001) 61–74

EPSL

www.elsevier.com/locate/epsl

A sedimentary paleomagnetic record of the Matuyama chron from the Western Antarctic margin (ODP Site 1101)

Yohan Guyodo^{a,*}, Gary D. Acton^b, Stefanie Brachfeld^{c,1},
James E.T. Channell^a

^a Department of Geological Sciences, University of Florida, Gainesville, FL, USA

^b Ocean Drilling Program, Texas A&M University, College Station, TX, USA

^c Institute for Rock Magnetism, University of Minnesota, Minneapolis, MN, USA

Received 25 January 2001; received in revised form 12 June 2001; accepted 12 June 2001

Abstract

A high-resolution paleomagnetic record for part of the Matuyama chron (0.7–2.1 Ma) is reported for Ocean Drilling Program Site 1101 (Leg 178), off the Antarctic Peninsula Pacific margin. A rock-magnetic investigation of 62 discrete samples revealed that the natural remanent magnetization (NRM) is carried by pseudo-single domain magnetite. Progressive alternating field demagnetization of 83 m of U-channels provided a polarity stratigraphy down to the Olduvai subchron. Two geomagnetic events preceding the Jaramillo subchron were identified, including the Cobb Mountain polarity interval. The bulk magnetic parameters vary by more than a factor of 20 over the entire time interval, but by less than a factor of 6 over the 0.7–1.1 Ma interval. This latter interval was selected for paleointensity determinations, which were carried out by normalizing the NRM by the anhysteretic remanent magnetization (ARM). Direct comparison of the Site 1101 paleointensity record with other curves available for the same time interval suggests a geomagnetic origin for features present in the record. A more quantitative comparison was achieved by means of a jackknife test performed on nine records of relative paleointensity over the 0.95–1.1 Ma interval. This test yielded no outlier for the period considered, confirming the geomagnetic character of the records. We have constructed a low-resolution stack revealing some of the characteristic paleointensity features of the Jaramillo subchron. © 2001 Elsevier Science B.V. All rights reserved.

Keywords: paleomagnetism; magnetostratigraphy; magnetic intensity; Antarctic Peninsula

1. Introduction

Our understanding of the geomagnetic field has increased tremendously owing in part to rapid advances in paleomagnetic techniques and technology, which have facilitated the acquisition of reliable continuous records of relative paleointensity from marine sediments (e.g. [1–15]). The growing interest in establishing sedimentary

* Corresponding author. Tel.: +1-352-392-2231;

Fax: +1-352-392-9294.

E-mail address: guyodo@ufl.edu (Y. Guyodo).

¹ Present address: Byrd Polar Research Center, Ohio State University, Columbus, OH, USA.

paleointensity records has led to the development of compilations aimed at describing the time evolution of dipole field intensity, as well as providing new stratigraphic correlation tools [16–18]. Most of the studies that have been published in the past 20 years were limited to low and middle latitudes, with only a few from the high latitudes of the Northern Hemisphere [1–3,18,19]. To establish the global character of the dipole field variations, it is important to obtain paleointensity records from high latitudes in the Southern Hemisphere. The only relative paleointensity records from mid or high latitude Southern Hemisphere are from the subantarctic South Atlantic [20]. These records can be correlated among several sites, and to records from the Northern Hemisphere, for the last 100 kyr [20,11]. More sedimentary paleointensity records from high latitude sites are needed to understand the long-term evolution of the geodynamo, to study spatial and temporal variations in the strength of the field over periods of constant geomagnetic polarity, and to examine how the field regenerated following polarity reversals [6,15,21–24].

In this paper, we present a geomagnetic record derived from sediments collected on drift deposits off the Western Antarctic Peninsula continental margin, at Ocean Drilling Program (ODP) Site 1101 (Leg 178). This record provides a magnetostratigraphy down to 2.1 Ma, and a record of relative paleointensity for the period 0.7–1.1 Ma. This high latitude, Southern Hemisphere paleointensity record is aimed at improving the statistical robustness of the database available for this period of time.

2. Geological setting and lithology

ODP Site 1101 (64°22'S, 70°16'W, 3509 m water depth) is located at the crest of a sediment drift on the continental rise of the Antarctic Peninsula Pacific margin (Fig. 1). This drift is part of a series of eight large hemipelagic sediment drifts (about $130 \times 50 \times 1$ km³ in dimension), which are interpreted to have resulted from the interaction between turbidity currents and bottom currents at the base of the continental slope [25]. The drifts

are separated by large channels (up to 5 km wide) formed by turbidity currents that transport sediment from the lower continental slope toward the abyssal plain [26]. Part of the fine-grained fraction of those turbidity currents is entrained in a bottom current nepheloid layer. The drifts are constructed above the level of turbidity flow by the down-current deposition of fine-grained suspended material [25]. During ODP Leg 178, the sediment was collected by advanced piston corer (APC) down to 142.7 mbsf (meters below sea floor), then cored with the extended core barrel (XCB) technique down to 217 mbsf [27]. The recovered sedimentary sequence consisted essentially of hemipelagic clayey silt, and was divided into three lithological units during shipboard analyses [27]. Unit I (0–53 mbsf) comprises alternations of laminated and massive clayey silts that are interpreted as the expression of glacial and interglacial periods, respectively. In this unit, the intervals corresponding to warm periods are indicated by the presence of diatom-bearing layers. Similar alternations were observed in the underlying unit (Unit II, 53–142.7 mbsf), but here the warm intervals are characterized by foraminifera-bearing layers. The laminated facies of Unit II is characterized by mm-thick bioturbated silty clay laminations, which appear as subtle color banding. They suggest a low-energy depositional setting dominated by weak bottom contour currents [27]. As in Unit I, the faint laminations are interpreted as resulting from deposition of the fine-grained fraction of the suspended sediment load associated with turbidity currents [27]. The third unit (Unit III, 142.7–217.7 mbsf) does not display the cyclic pattern observed in Units I and II, and is mostly composed of massive clayey silts that probably originated from the deposition of turbidities, and ice-rafted debris.

We have sampled the depth interval 50–133 mbsf using 5 cm³ cylinders (at ~1 sample per core section) and U-channel samples (shore-based continuous sampling). This depth interval corresponds roughly to lithologic Unit II. Only one APC hole was cored at Site 1101, so that no composite section is available at this site and small parts of the geological record may be missing. In the unit sampled, laminated intervals alternate

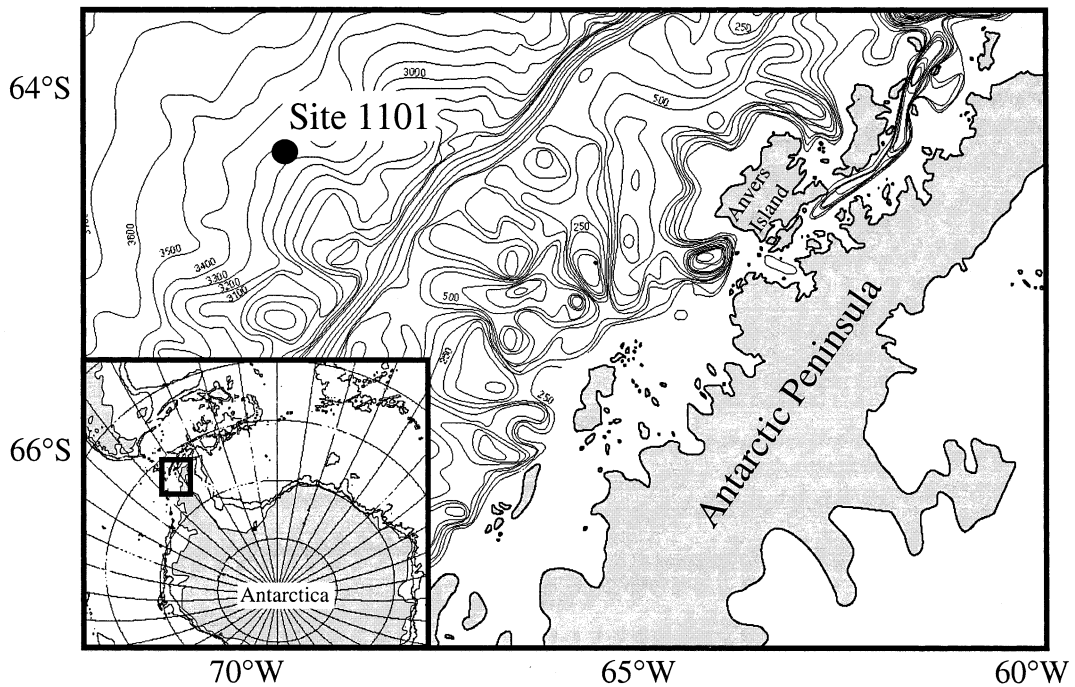


Fig. 1. Location map for ODP Site 1101, on the western margin of the Antarctic Peninsula.

with massive intervals. These mm-scale laminations are subtle variations within a fairly homogeneous silty clay or clayey silt unit. The thickness of the laminations is an order of magnitude smaller than the ~ 4 cm response function of the magnetometer used in this study. Occasionally, sharp-based, 1–3 mm silt laminations are present, probably induced by distal low-density turbidity flows. A few thicker layers, ranging from 0.5 to 4 cm in thickness are also present in the sequence at 66, 87.5, 116.7, and 136.8 mbsf. These are associated with high frequency peaks in the ship-board magnetic susceptibility data [27], and therefore have been omitted from further study. The massive intervals, attributed to warmer periods, are characterized by lower values of magnetic susceptibility, probably due to biogenic dilution of the terrigenous input [27].

3. Magnetic mineralogy and grain size

We measured the hysteresis properties and low-temperature demagnetization of the discrete sam-

ples at the Institute for Rock Magnetism at the University of Minnesota. The hysteresis parameters were measured on a Princeton Measurements Corporation micro-VSM. The low-temperature remanence properties were measured on a Quantum Design Magnetic Properties Measurement

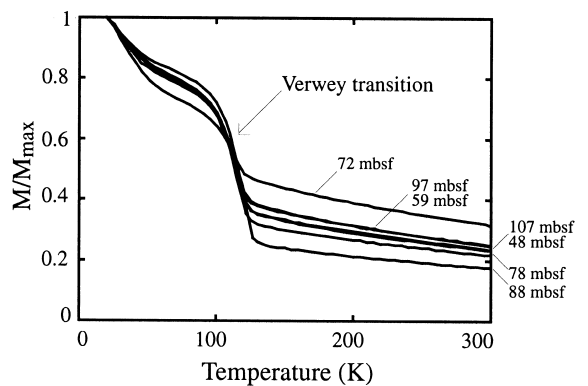


Fig. 2. Thermal demagnetization at low temperature of the saturation isothermal remanent magnetization imparted at 20 K on seven samples collected at Site 1101. The remanence loss at 110–120 K indicates the Verwey transition for magnetite.

System (MPMS). The low-temperature measurements performed on seven samples (randomly selected from 48 to 107 mbsf) show a significant drop in the intensity of magnetization around 110–120 K, corresponding to the Verwey transition of magnetite (Fig. 2). No other low-temperature transition was observed. This indicates that magnetite is the main mineral carrier of the magnetization in these sediments (Fig. 2). The hysteresis loops obtained for 62 gelatin capsule samples have been compiled in Fig. 3a. The shape of these hysteresis loops, as well as the values of the coercivity are compatible with those of magnetite. Calculation of the coercivity of remanence over coercivity (H_{cr}/H_c) and saturation remanence

over saturation magnetization (M_{rs}/M_s) indicates a pseudo-single domain state for the magnetite grains [28] (Fig. 3b), except for one sample which is located in the multi-domain field on a ‘Day-plot’ (Fig. 3b). This sample (122.45 mbsf) was taken from an interval containing coarser-grained ice-rafted debris (IRD).

4. Magnetostratigraphy

The natural remanent magnetization (NRM) of the U-channel samples was measured at 2-cm intervals and was stepwise alternating field (AF) demagnetized at 20, 30, 40, 50, 60, and 80 mT peak values, using the 2-G Enterprises magnetometers located at the Institut de Physique du Globe de Paris and at the University of Florida. The viscous component of magnetization was successfully removed by treatment at 20 mT, and the progressive AF demagnetization provided data of sufficient quality to define reliable directions of magnetization for the entire sedimentary sequence investigated (Fig. 4). We used the standard least-squares method to determine the principal components of paleomagnetic directions defined in the 20–80 mT interval [29]. Unfortunately, the declination was not azimuthally oriented during drilling. The paleomagnetic inclination is, however, sufficient to establish a clear succession of polarity zones down to below the Olduvai subchron (Fig. 5). The distribution of inclination values is bimodal, with two maxima located at -75° (normal polarity) and $+78^\circ$ (reverse polarity), which are close to the values of $\pm 76.5^\circ$ expected for a geocentric axial dipole field for a site at this latitude. Values of the maximum angular deviation (MAD) associated with our calculation of the principal components are for the most part lower than 5° , which demonstrates the overall quality of the directional data. The Brunhes/Matuyama polarity reversal occurs at 54.99 mbsf, the Jaramillo subchron is present over the interval 70.96–76.15 mbsf, and the Olduvai subchron is recorded between 121.25 and 126.97 mbsf. These depths are similar to those determined during shipboard investigations [27].

We also observed two thin intervals with anom-

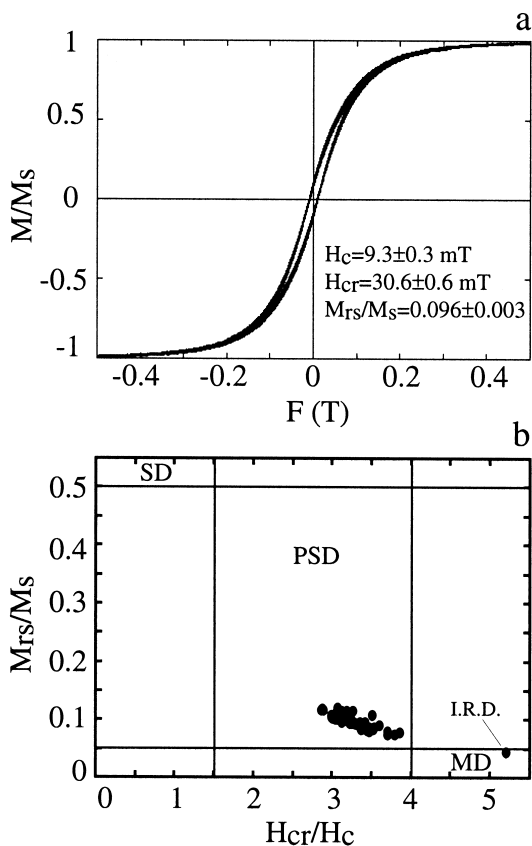


Fig. 3. (a) Hysteresis loops for 62 samples collected at Site 1101. The magnetic moments are normalized by their values at saturation. (b) Magnetic grain size distribution, as indicated by variations in the hysteresis parameters [28]. SD, single domain; MD, multi-domain; and PSD, pseudo-single domain. IRD, ice-rafted debris.

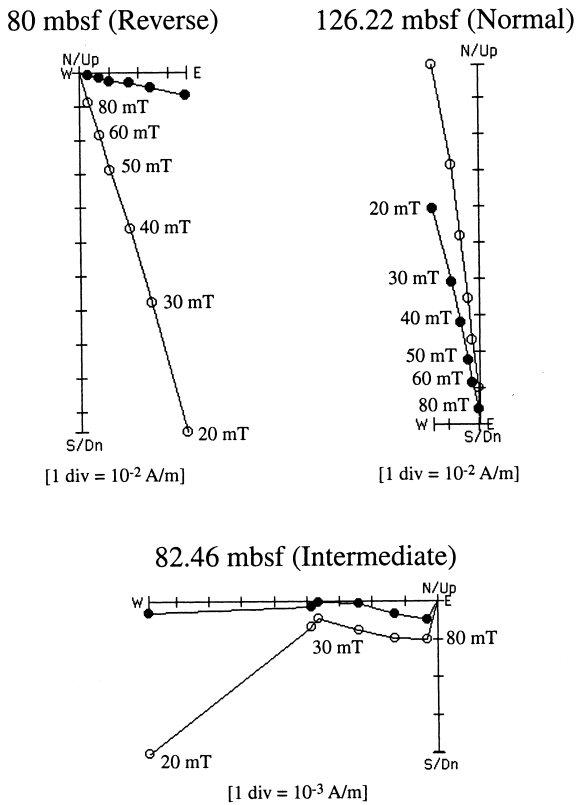


Fig. 4. Typical examples of orthogonal projection (Zijderveld) plots for samples taken in reverse and normal polarity intervals, and during a polarity reversal. Open and closed symbols represent projections of vector endpoints onto the vertical and horizontal planes, respectively. The plots show clear single-component directions of the NRM during periods of stable polarity, and no apparent drilling overprint after demagnetization at 20 mT.

alous directions below the Jaramillo subchron (at 77.2–78.5 mbsf and 80.9–82.5 mbsf), hereafter referred to as Event 1 and Event 2 (Fig. 5). Using a linear interpolation from the base of the Jaramillo subchron (1.07 Ma) to the top of the Olduvai subchron (1.77 Ma) [30], we obtained ages of 1.09–1.11 Ma for Event 1 and 1.14–1.17 Ma for Event 2. Event 2 is likely to be the Cobb Mountain polarity interval, for which Shackleton et al. [31] gave an age of 1.19 Ma by correlation of ODP Site 677 and DSDP Site 609. A similar succession of events has been observed in sediments from the California margin [14], where the event between the Cobb Mountain and the Jaramillo

subchrons has been attributed to the Punaruu event, originally recorded in three lava flows from the Punaruu Valley in Tahiti [32]. Our study suggests that two short geomagnetic events preceded the onset of the Jaramillo subchron at least locally over the Antarctic Peninsula, with a timing similar to the succession of events recorded in the Pacific [14].

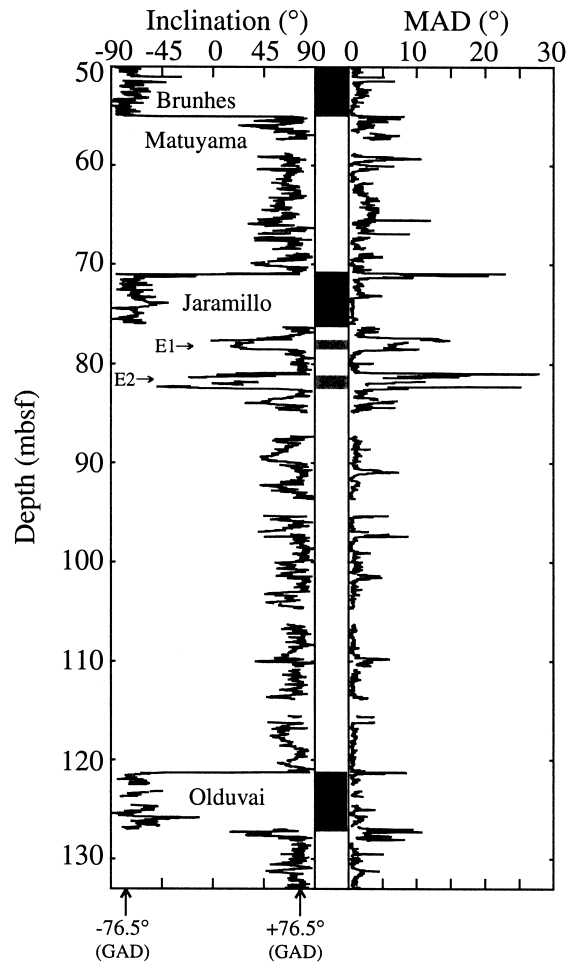


Fig. 5. Inclination variations and maximum angular deviation (MAD) at Site 1101. Values of the MAD are generally lower than 5°, except during polarity transitions and short polarity intervals (E1, Event 1; E2, Event 2). The geocentric axial dipole (GAD) field inclinations for the site latitude ($\pm 76.5^\circ$) are also shown.

5. Time scale

Oxygen isotope analysis was not possible at Site 1101 due to the overall low biogenic carbonate content, thus constraining us to date these sediments by other means. An initial time scale was derived from the magnetostratigraphy (Fig. 5), using the ages of Cande and Kent [30]. This yielded mean sedimentation rates of 8.8 cm/kyr for the period 0.7–0.99 Ma, and of 6.1 cm/kyr for the period 0.9–2.1 Ma. A lower sedimentation rate of 3.1 cm/kyr was found for the Olduvai subchron, suggesting the possible presence of a hiatus or at least large variations in sedimentation rates in this interval. Considering the depositional setting in this region, the sedimentation rates are probably variable throughout the cored interval, possibly varying on a glacial/interglacial time scale.

Shipboard analyses showed that part of the magnetic susceptibility (κ) variations could be related to changes in the silica and carbonate content of the sediment, because susceptibility minima were generally associated with intervals of higher biogenic content [27]. This suggests that κ is primarily responding to variable dilution of terrigenous material with biogenic material. Conse-

quently, because the biogenic content at Site 1101 varies with climatic periods [27], first-order variations of the U-channel magnetic susceptibility (κ) should correlate with climatic proxies. Therefore, we have refined our time scale by correlating the magnetic susceptibility to the benthic $\delta^{18}\text{O}$ target curve of ODP Site 677 [31]. The correlation is shown in Fig. 6, along with the location of CaCO_3 maxima, which indicate warmer periods [27]. The major variations displayed by the susceptibility record can be matched fairly accurately to the $\delta^{18}\text{O}$ record, although uncertainties remain over shorter time scales.

6. Relative paleointensity

6.1. Choice of the normalizing parameter

The bulk magnetic parameters were measured at 2-cm stratigraphic intervals using 2-G Enterprises cryogenic magnetometers located in shielded rooms in the paleomagnetic laboratories at the University of Florida and at the Institut de Physique du Globe de Paris. An anhysteretic remanent magnetization (ARM) was imparted to the U-channel samples using a peak AF of

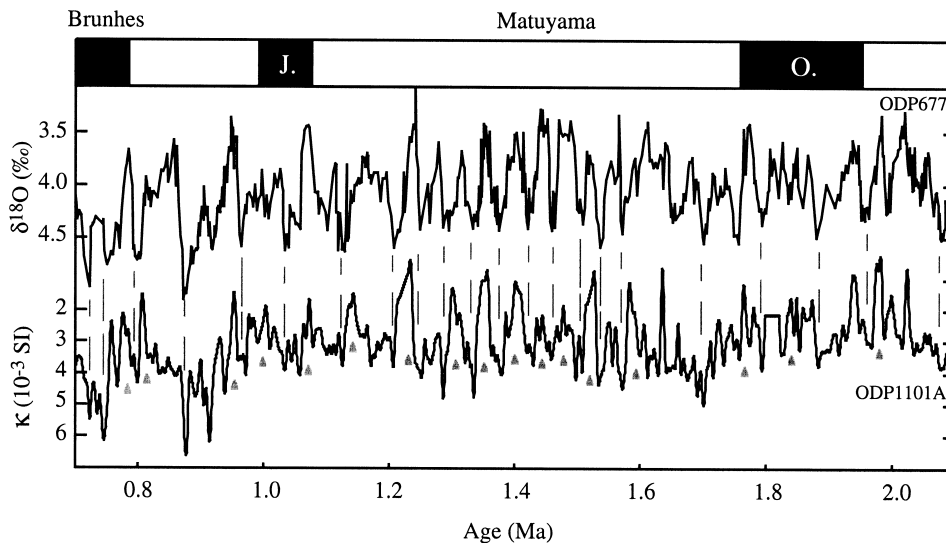


Fig. 6. Correlation of the U-channel magnetic susceptibility record from Site 1101 to the benthic $\delta^{18}\text{O}$ record from ODP Site 677 [31]. The correlation is suggested by gray lines. The gray triangles indicate the stratigraphic location of warmer climatic intervals inferred in part from peaks in the shipboard CaCO_3 record [27].

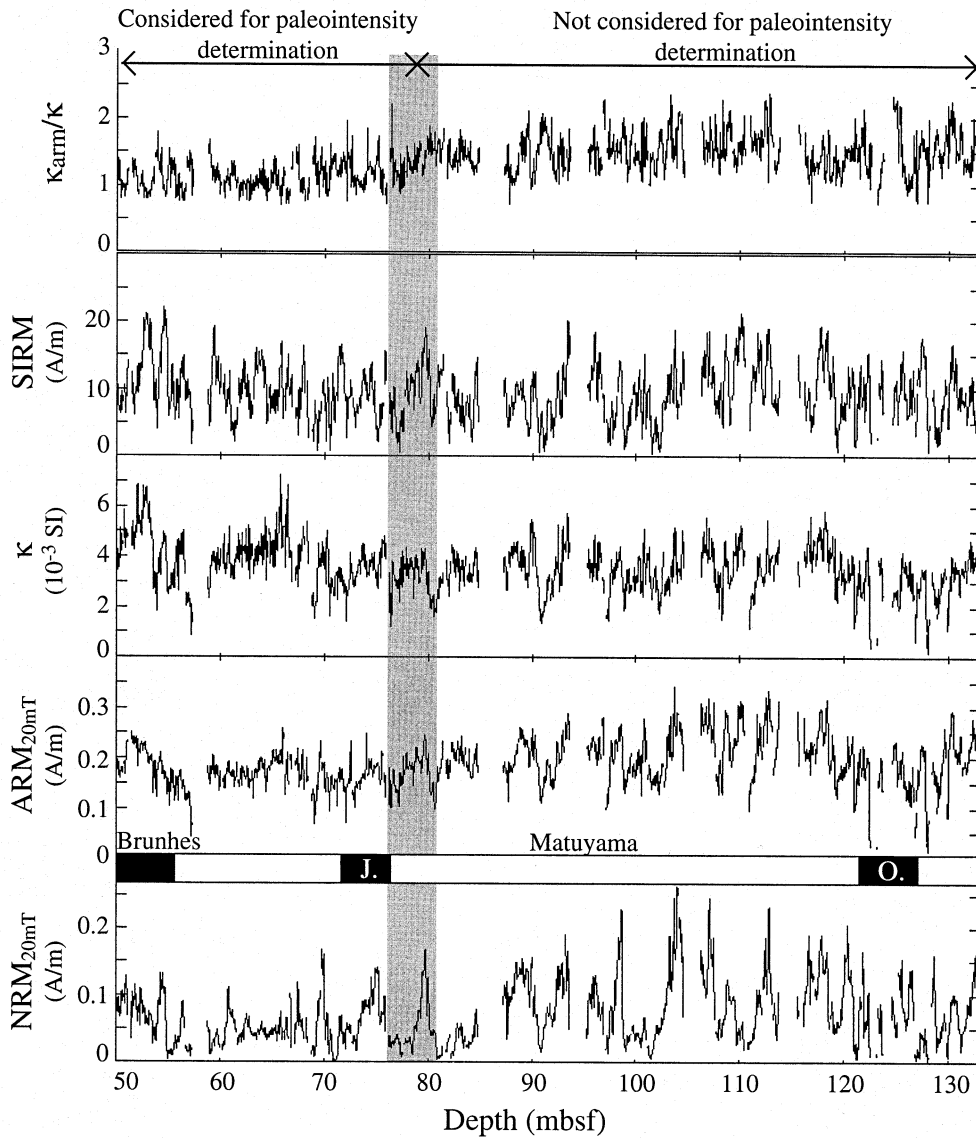


Fig. 7. Bulk magnetic parameters for Site 1101. From bottom to top: down-core variations of the NRM demagnetized at 20 mT, ARM demagnetized at 20 mT, κ , SIRM, and $\kappa_{\text{arm}}/\kappa$. Overall, ARM varies by a factor greater than 20, which is more than usually considered acceptable for paleointensity determinations [33]. Over the interval 50–78 mbsf, however, ARM varies by less than a factor of 6, within the acceptable range.

100 mT and a 0.05-mT DC bias field, and subsequently was demagnetized at peak fields of 20, 30, 40, and 60 mT. The ratio of the susceptibility of ARM (κ_{arm} , ARM normalized by the bias field) over magnetic susceptibility (κ) was subsequently computed. When dealing with magnetite, $\kappa_{\text{arm}}/\kappa$ varies inversely with magnetic grain size,

and so can be used to monitor down-core changes in magnetic grain size. In addition, a saturation isothermal remanent magnetization (SIRM) was imparted using a 1 T field.

The down-core variations of these parameters are shown in Fig. 7. ARM, κ , and SIRM are believed to primarily reflect down-core changes

in concentration of magnetic particles in the sediment (e.g. [33]). It has been proposed that bulk magnetic parameters should vary by less than an order of magnitude in order to obtain useful paleointensity proxies (e.g. [33,34]), which is not the case in the present study. For instance, ARM values vary by almost a factor of 20 throughout the entire record. However, most of this variability is due to large amplitude changes below 78 mbsf, where there is a 50% down-core increase of the mean value of the NRM. The interval between 50 and 78 mbsf contains less variability in NRM intensity than the underlying sediment. This change is also seen to some extent in the $\kappa_{\text{arm}}/\kappa$ ratio, which indicates a slightly finer average grain size for the interval 78–133 mbsf. These changes are probably sufficient to induce a shift in the response of remanence parameters to the applied field, and therefore these two depth intervals should be treated separately. In addition, the lower interval (78–133 mbsf) contains more regions of sediment disturbance (essentially at the top of cores), which make it difficult to obtain a complete geomagnetic record for this part of the record. For the study of relative paleointensity at Site 1101, we consequently restricted our investigation to the depth interval between 50 and 78 mbsf. Over this interval, the ARM varies by less than a factor of 6, which is appropriate for paleointensity determinations [33].

6.2. Relative paleointensity

In order to construct a relative paleointensity

record, one must correct for variations in concentration of remanence (NRM) carrying grains. This is done by selecting the magnetic parameter (i.e. ARM, κ , or SIRM), that provides the best measure of the concentration of the magnetic grains that carry the NRM. We attempt to ascertain this using coherence functions between the magnetic parameters (ARM, κ , and SIRM) and the paleointensity determined from normalizing the NRM by these parameters (Fig. 8). In principle, when the normalization is appropriate, the relative paleointensity is not correlated to the bulk rock-magnetic parameter used to normalize the NRM, and the values of the coherence should be lower than the 95% confidence level [33]. Squared coherence values lie above the confidence level over specific frequency intervals for the susceptibility normalization (Fig. 8b). Much higher values of the squared coherence, and more spread over the frequency domain, are found for the SIRM normalization. Some problems were encountered when measuring the SIRM, due to the fact that the dynamic range of the magnetometer was sometimes exceeded when the intensity gradient was large. Therefore, some caution should be used when dealing with SIRM magnetization at this site. The lowest squared coherence occurs for the ARM normalization, indicating that it is the best choice, even though there are some frequency intervals over which the coherence is close to the significance level. The use of ARM as the normalizer can be further validated by comparing paleointensity estimates obtained with the ratios $\text{NRM}_{20}/\text{ARM}_{20}$, $\text{NRM}_{30}/\text{ARM}_{30}$,

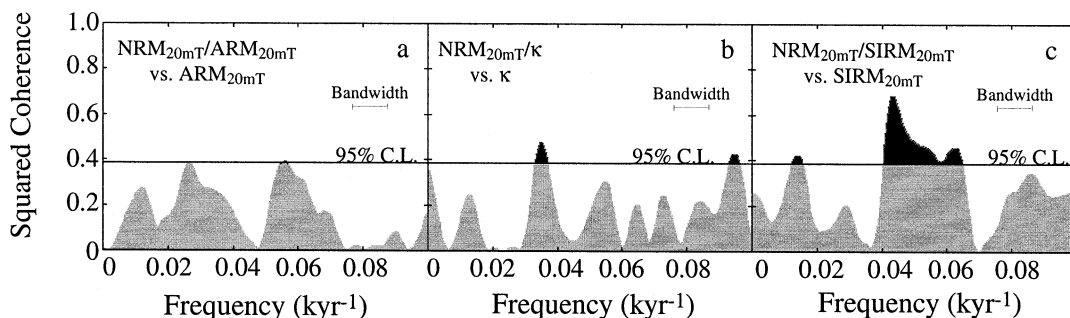


Fig. 8. Coherence function between (a) ARM, (b) κ , and (c) SIRM, and the paleointensity proxies obtained by normalizing the NRM with these parameters for the interval 50–70 mbsf. Coherence above the 95% confidence values level are shown in black.

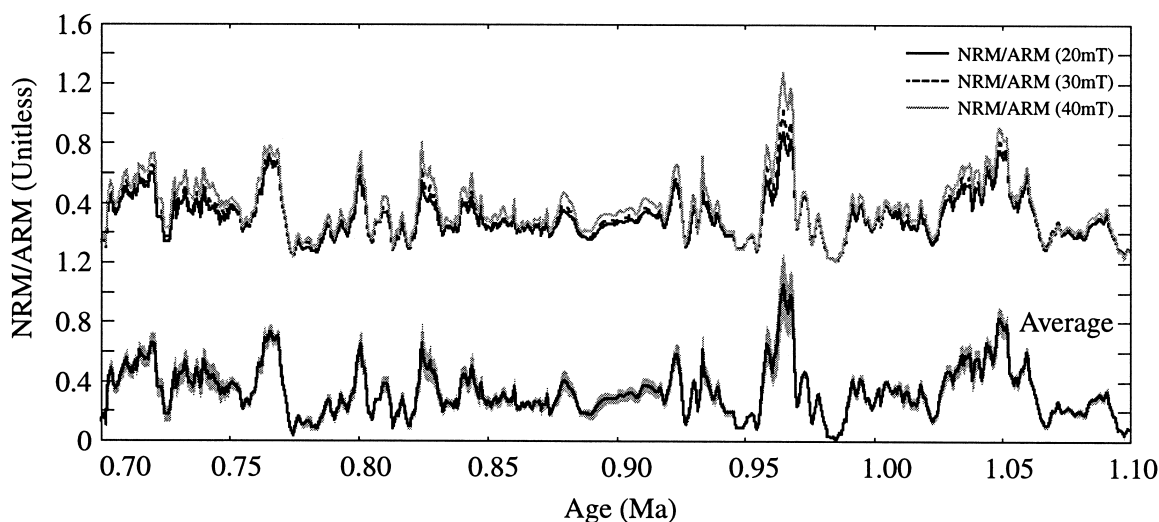


Fig. 9. Paleointensity proxies obtained by dividing the NRM demagnetized at 20, 30, and 40 mT by ARM demagnetized at 20, 30, and 40 mT (top), and the arithmetic mean of the three normalizations (bottom). The standard deviation associated with the mean is plotted in gray.

and $\text{NRM}_{40}/\text{ARM}_{40}$ (Fig. 9). They show nearly identical variations, which confirm the match between the coercivity spectra of the ARM and the NRM over the range of peak AFs. Therefore, we consider the ratio NRM/ARM to provide the best estimate of relative paleointensity at Site 1101. We used the average of the three ARM normalizations as our paleointensity proxy (Fig. 9).

7. Comparison with other paleointensity records

One way of verifying the overall quality of a sedimentary paleointensity record is to compare it with other paleointensity curves available for the same time interval. In Fig. 10, the paleointensity record obtained at ODP Site 1101 is compared with a record obtained at ODP Site 983 (ODP983) [3] and a compilation from the Pacific Ocean (VM93) [15]. The long-term features present in the paleointensity record at Site 1101 are also observed in the two other paleointensity records. All records show a relatively sharp increase in the paleointensity after the geomagnetic reversals at the onset and termination of the Jaramillo subchron, and at the onset of the Brunhes chron. Overall, most of the variations with wave-

lengths of the order of a few tens of thousand years can be correlated between Sites 1101 and 983 (Fig. 10). The correlation is poorer with VM93, and is also less easy to establish between ~ 0.82 Ma and ~ 0.9 Ma. The high-frequency variations are more difficult to correlate from one record to another, due to differences in the resolution and possible time scale discrepancies between records.

Most of the long-term variations seen in contemporaneous paleointensity records from the North Atlantic and Pacific oceans are reproduced by our paleointensity record, and the main differences seem to appear as amplitude modulations of the paleointensity. Therefore, we attribute a common geomagnetic origin to the features observed in our paleointensity record. Some of the differences with other records could be due to failure in removing some of the non-geomagnetic signal present in the record, or uncertainties in chronologies [16,35,36]. The best approach is probably to compare our record with a database integrating paleointensity records of resolution comparable with that at Site 1101, and corresponding to different regions of the globe and to different lithologies. This type of comparison is tenuous for the 0.7–1.1 Ma interval, because few records exist

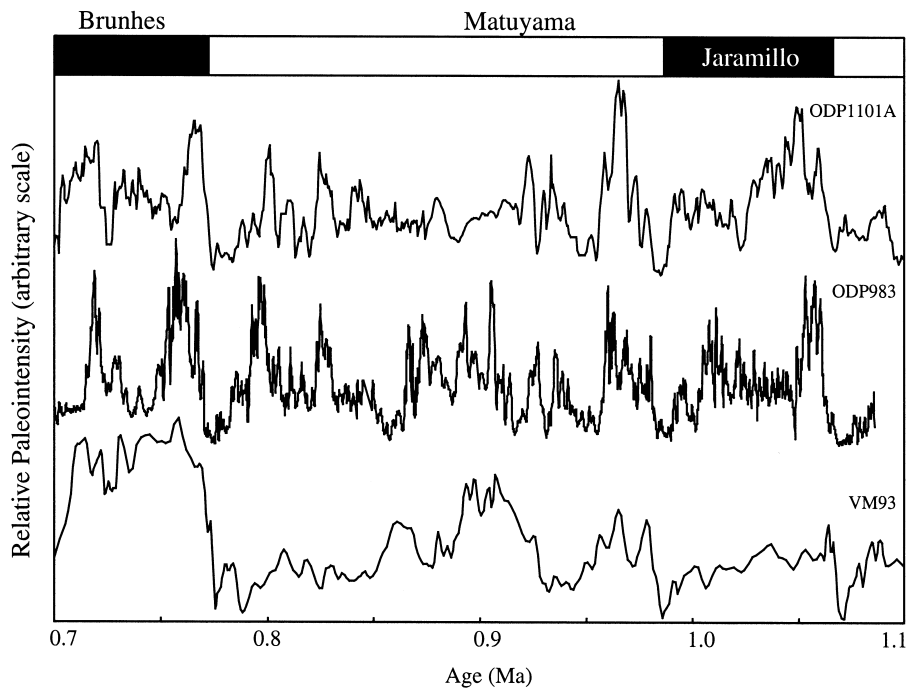


Fig. 10. Comparison of the paleointensity profile obtained at Site 1101 with previously published records from the North Atlantic [1–3] and the Pacific [15] oceans.

with reasonably good age control. However, some answers may be provided by a study of the short interval 0.95–1.1 Ma, which includes the Jaramillo subchron. This interval is characterized by sharp paleointensity features, and a time scale that is relatively well constrained by the presence of two geomagnetic reversals.

Nine paleointensity records corresponding to different sedimentary environments are shown in Fig. 11. There are six sites located in the Pacific Ocean (ODP1021, [14]; VM93, [15]; S98, [37]; ODP1010C, [38]; KK78030, [39,40]; KT99 [41]), one in the Indian Ocean (MD940, [6]), one in the Atlantic Ocean (ODP983, [3]), and Site 1101. Most of these records show similar variations with minima that are synchronous within a few thousand years, although the amplitudes of specific peaks may vary from one record to another. Before performing a quantitative comparison, it is important to reduce the discrepancies related to resolution and dating. Over the time period considered, some of these curves have been dated solely by magnetostratigraphy (ODP1010C,

KK78030, ODP1021, S98, KT99), others by correlation of indirect climatic proxies to target curves (VM93, MD940, ODP1101), and only one using oxygen isotope techniques (ODP983). This leaves some margin for small readjustments of the age models for individual records. The age model for ODP983 [3] was derived from the tuning of precession cycles present in its $\delta^{18}\text{O}$ record to those of the ice volume model of Imbrie and Imbrie [42], and this paleointensity record probably has the highest resolution chronology. For this reason, we correlated the major geomagnetic features of all the paleointensity records to core ODP983. We tied the records using correlation points near the polarity reversals (Fig. 11b), maintaining a consistent age for the two reversals at the boundaries of the Jaramillo subchron, where the intensity changes are the most dramatic. Other paleointensity features could have been matched, but the legitimacy of such a procedure would have been difficult to assess without the existence of independent control (i.e. oxygen isotope data). We also resampled the data every 1 kyr to obtain

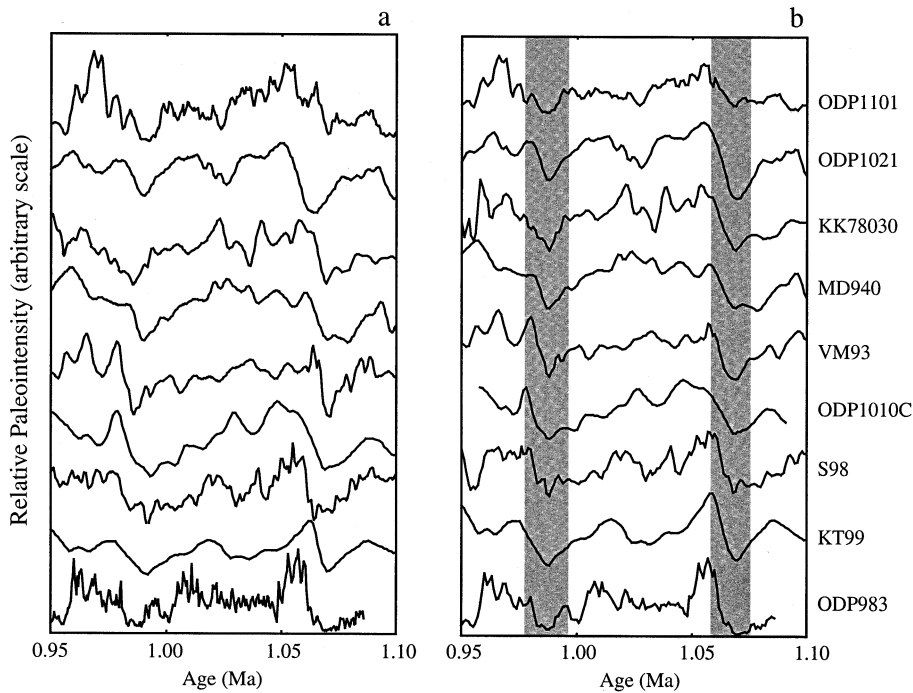


Fig. 11. (a) Relative paleointensity at Site 1101 compared with eight other records over the time interval 0.95–1.1 Ma (ODP1021, [14]; KK78030, [39,40]; MD940, [6]; VM93, [15]; ODP1010C, [38]; S98, [37]; KT99, [41]; ODP983, [3]). All the records are placed on their published age models. (b) The same records after minor readjustment of the time scales around the reversals (in gray). The time scale of core ODP983 was taken as the reference. The records in (b) have been resampled at 1 kyr intervals.

an even time sampling and to reduce the differences in resolution (although some differences remain), and normalized the data to equal mean and variance over the time interval common to all the records (0.958–1.086 Ma). The results of this operation are shown on Fig. 11b, which is similar to Fig. 11a.

A suitable procedure for evaluating the degree of reliability of specific records involves comparing each paleointensity record to the rest of the database. One statistical approach would be to perform a test similar to a jackknife. In order to do so, and to evaluate the amount of noise introduced by each of the nine paleointensity records in our database, we built nine distinct subsets of data, each time removing a different record from the database. For each subset of eight records, we calculated the relative difference between the average curve calculated with this particular subset and a reference curve constructed with all the

records (Fig. 12a, hereafter referred to as the Jaramillo Stack). This difference provides a measure of the bias introduced by the record that was removed from the database. If a significant change is noticed in the average curve when a specific record is removed from the database, it means that this record has a negative impact on the stack, and therefore does not fit well to the other records. The nine paleointensity curves obtained by following this procedure are plotted in Fig. 12b. From this figure, it is not possible to distinguish any outlier. The minimum difference between the average curves obtained with the nine subsets and the Jaramillo Stack was found with core KK78030 ($1.0 \pm 0.2\%$). The maximum difference was obtained with core KT99 ($1.5 \pm 0.2\%$) (Table 1). In addition, we calculated the correlation coefficients between the individual paleointensity records and the Jaramillo Stack. All the correlation coefficients are greater than

0.8 (Table 1), which indicates a strong correlation between the records, and attests to their geomagnetic origin.

8. Conclusions

We have investigated the magnetic properties of a sedimentary sequence at ODP Site 1101 covering the time interval 0.7–2.1 Ma. The NRM of the sediment is carried by pseudo-single domain magnetite, and yielded a directional record allowing us to establish a magnetostratigraphy down to the Olduvai subchron. In the sediment underlying the Jaramillo subchron, two short geomagnetic events were observed at 1.09–1.11 Ma (Event 1) and 1.14–1.17 Ma (Event 2). Event 2 is identified as

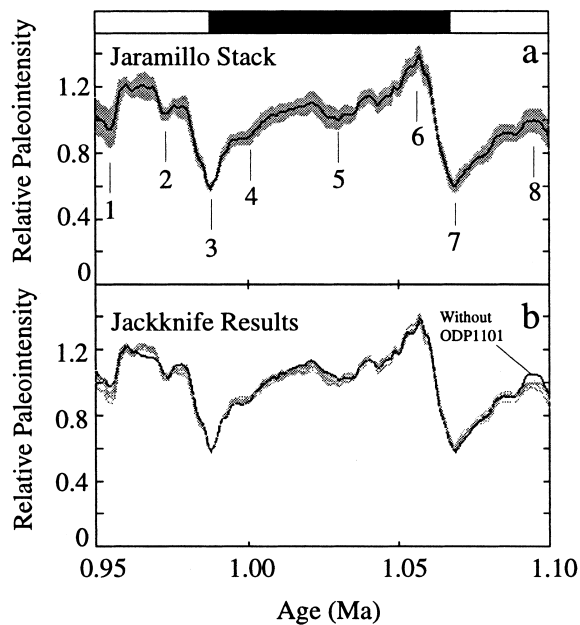


Fig. 12. Results of the jackknife test performed on the paleointensity records shown in Fig. 11. (a) Reference curve for the test. This curve corresponds to the arithmetic mean of the nine records in Fig. 11b. The error bars (in gray) correspond to the standard error. The characteristic features of this stack are labeled with numbers. (b) Jackknife results showing the nine stacks obtained from nine subsets of paleointensity records. Each subset is obtained by removing a different record from the entire database. The result corresponding to the subset without core ODP1101 is shown in black. No outlier can be identified.

Table 1

Compilation of the average differences between the Jaramillo Stack and the stacks (delta) calculated from nine subsets of paleointensity records.

Paleointensity records	Delta (%)	<i>R</i>
ODP1101	1.3 ± 0.2	0.8
ODP1021	1.2 ± 0.2	0.9
VM93	1.3 ± 0.2	0.8
ODP983	1.1 ± 0.1	0.9
MD940	1.2 ± 0.2	0.8
S98	1.1 ± 0.1	0.9
ODP1010C	1.3 ± 0.1	0.8
KK78030	1.0 ± 0.2	0.9
KT99	1.5 ± 0.2	0.8

The uncertainties correspond to the standard error at the 95% level. Correlation coefficients (*R*) between individual paleointensity records and the Jaramillo Stack.

the Cobb Mountain polarity interval. Event 1, which occurred closer to the onset of the Jaramillo subchron, may be the same event as that observed on the California margin (Pacific Ocean, Site 1021) and in the Punaruu Valley, Tahiti.

We obtained a record of relative paleointensity by normalizing the NRM with the ARM after demagnetization at 20, 30, and 40 mT, over the time interval 0.7–1.1 Ma. Comparison of the paleointensity record obtained at ODP Site 1101 with records from the North Atlantic and Pacific oceans indicated that the variations recorded at Site 1101 are geomagnetic in origin. The quality of the record was additionally assessed by a jackknife test over the time interval 0.95–1.1 Ma. This enabled construction of a composite record of relative paleointensity for the Jaramillo subchron, by compiling the geomagnetic features common to nine sites from different oceans (Fig. 12a). Overall, the Jaramillo Stack displays the same variations as those documented in previous studies (e.g. [3,38,39]) (Fig. 12a). The paleointensity variations can be correlated from one hemisphere to the other for this time interval, although features may vary in amplitude from one record to another. They reflect global variations of the geomagnetic dipole over the time span investigated here. Better definition of these features could be achieved by slightly shifting the individual records within the Jaramillo subchron, but the validity of such a procedure cannot be established with the

existing age control. Paleointensity minima numbered 3 and 7 in Fig. 12a are the most prominent features of this compilation, and correspond to the polarity reversals bounding the Jaramillo subchron. Recovery of field intensity post-reversal is abrupt and appears to occur within ~ 15 kyr. Additional records, with better age control and higher resolution will be needed in order to reduce the error bars, and extend the time domain explored by this type of compilation. With this in mind, the recovery of complete and well-dated sedimentary sequences from high latitudes will be crucial for developing the database necessary to test the various geodynamo models.

Acknowledgements

We are grateful to A.P. Roberts and T. Yamazaki for their reviews of the manuscript, and to T. Sato who provided us with data. We thank the Ocean Drilling Program for providing access to the Site 1101 cores. This research was supported in part by grants from the JOIDES U.S. Science Support Advisory Committee (USSAC) and from the National Science Foundation (OCE97-11424). The Institute for Rock Magnetism is funded by the Keck Foundation, the National Science Foundation, and by the University of Minnesota. *[RV]*

References

- [1] J.E.T. Channell, D.A. Hodell, B. Lehman, Relative geomagnetic paleointensity and $\delta^{18}\text{O}$ at ODP Site 983 (Gardar Drift, North Atlantic) since 350 ka, *Earth Planet. Sci. Lett.* 153 (1997) 103–118.
- [2] J.E.T. Channell, D.A. Hodell, J. McManus, B. Lehman, Orbital modulation of geomagnetic paleointensity, *Nature* 394 (1998) 464–468.
- [3] J.E.T. Channell, H.F. Kleiven, Geomagnetic palaeointensities and astrochronological ages for the Matuyama-Brunhes boundary and the boundaries of the Jaramillo Subchron: palaeomagnetic and oxygen isotope records from ODP Site 983, *Philos. Trans. R. Soc. Lond. A* 358 (2000) 1027–1047.
- [4] E. Tric, J.-P. Valet, P. Tucholka, M. Paterne, L. Labeyrie, F. Guichard, L. Tauxe, M. Fontugne, Paleointensity of the geomagnetic field for the last 80,000 years, *J. Geophys. Res.* 97 (1992) 9337–9351.
- [5] L. Meynadier, J.-P. Valet, R. Weeks, N.J. Shackleton, V.L. Hagee, Relative geomagnetic intensity of the field during the last 140 ka, *Earth Planet. Sci. Lett.* 114 (1992) 39–57.
- [6] L. Meynadier, J.-P. Valet, F.C. Bassinot, N.J. Shackleton, Y. Guyodo, Asymmetrical saw-tooth pattern of the geomagnetic field intensity from equatorial sediments in the Pacific and Indian Oceans, *Earth Planet. Sci. Lett.* 126 (1994) 109–127.
- [7] L. Tauxe, N.J. Shackleton, Relative paleointensity records from the Ontong-Java plateau, *Geophys. J. Int.* 117 (1994) 769–782.
- [8] T. Yamazaki, N. Ioka, N. Eguchi, Relative paleointensity of the geomagnetic field during the Brunhes Chron, *Earth Planet. Sci. Lett.* 136 (1995) 525–540.
- [9] T. Yamazaki, Relative paleointensity of the geomagnetic field during the Brunhes Chron recorded in the North Pacific deep-sea sediment cores: orbital influence?, *Earth Planet. Sci. Lett.* 169 (1999) 23–35.
- [10] J.S. Stoner, J.E.T. Channell, C. Hillaire-Marcel, Late Pleistocene relative geomagnetic paleointensity from the deep Labrador sea: regional and global correlations, *Earth Planet. Sci. Lett.* 134 (1995) 237–252.
- [11] J.S. Stoner, J.E.T. Channell, C. Hillaire-Marcel, C. Kissel, Geomagnetic paleointensity and environmental record from Labrador Sea core MD95-2024: global marine sediment and ice core chronostratigraphy for the last 110 kyr, *Earth Planet. Sci. Lett.* 183 (2000) 161–177.
- [12] D.A. Schneider, G.A. Mello, A high-resolution marine sedimentary record of geomagnetic intensity during the Brunhes Chron, *Earth Planet. Sci. Lett.* 144 (1996) 297–314.
- [13] B. Lehman, C. Laj, C. Kissel, A. Mazaud, M. Paterne, L. Labeyrie, Relative changes of the geomagnetic field intensity during the last 280 kyear from piston cores in the Azores area, *Phys. Earth Planet. Inter.* 93 (1996) 269–284.
- [14] Y. Guyodo, C. Richter, J.-P. Valet, Paleointensity record from Pleistocene sediments (1.4–0 Ma) off the California Margin, *J. Geophys. Res.* 104 (1999) 22953–22964.
- [15] J.-P. Valet, L. Meynadier, Geomagnetic field intensity and reversals during the past four million years, *Nature* 366 (1993) 234–238.
- [16] Y. Guyodo, J.-P. Valet, Relative variations in geomagnetic intensity from sedimentary records: the past 200 thousand years, *Earth Planet. Sci. Lett.* 143 (1996) 23–36.
- [17] Y. Guyodo, J.-P. Valet, Global changes in intensity of the Earth's magnetic field during the past 800 kyr, *Nature* 399 (1999) 249–252.
- [18] C. Laj, C. Kissel, A. Mazaud, J.E.T. Channell, J. Beer, North Atlantic palaeointensity stack since 75 ka (NAPIS-75) and the duration of the Laschamp event, *Philos. Trans. R. Soc. Lond. A* 358 (2000) 1009–1025.
- [19] J.S. Stoner, J.E.T. Channell, C. Hillaire-Marcel, A 200 kyr geomagnetic chronostratigraphy for the Labrador Sea: Indirect correlation of the sediment record to SPEC-MAP, *Earth Planet. Sci. Lett.* 159 (1998) 165–181.
- [20] J.E.T. Channell, J.S. Stoner, D.A. Hodell, C.D. Charles,

- Geomagnetic paleointensity for the last 100 kyr from the sub-Antarctic South Atlantic: a tool for inter-hemispheric correlation, *Earth Planet. Sci. Lett.* 175 (2000) 145–160.
- [21] A. Mazaud, Sawtooth variation in magnetic intensity profiles and delayed acquisition of magnetization in deep sea cores, *Earth Planet. Sci. Lett.* 139 (1996) 379–386.
- [22] Y. Kok, L. Tauxe, Saw-toothed pattern of relative paleointensity records and cumulative viscous remanence, *Earth Planet. Sci. Lett.* 137 (1996) 95–99.
- [23] L. Meynadier, J.-P. Valet, Post-depositional realignment of magnetic grains and asymmetrical saw-toothed pattern of magnetization intensity, *Earth Planet. Sci. Lett.* 140 (1996) 123–132.
- [24] L. Meynadier, J.-P. Valet, Y. Guyodo, C. Richter, Saw-toothed variations of relative paleointensity and cumulative viscous remanence: testing the records and the model, *J. Geophys. Res.* 103 (1998) 7095–7105.
- [25] M. Rebesco, R.D. Larter, P.F. Barker, A. Camerlenghi, L.E. Vanneste, The history of sedimentation on the continental rise west of the Antarctic Peninsula, in: P.F. Barker, A.K. Cooper (Eds.), *Geology and Seismic Stratigraphy of the Antarctic Margin* (Pt. 2), *Am. Geophys. Union, Antarct. Res. Ser.* 71 (1987) 29–50.
- [26] J.S. Tomlinson, C.J. Pudsey, R.A. Livermore, R.D. Larter, P.F. Barker, Long-range side scan sonar (GLORIA) survey of the Antarctic Peninsula Pacific Margin, in: Y. Yoshida, K. Kaminuma, K. Shiraiishi (Eds.), *Recent Progress in Antarctic Earth Science*, *Terra Sci. Publ.*, Tokyo (1992) 423–429.
- [27] Shipboard Scientific Party, Site 1101, in: P.F. Barker, A. Camerlenghi, G.D. Acton, et al., *Init. Rep. Proc. Ocean Drill. Prog.* 178 (1999) 1–83.
- [28] R. Day, M.D. Fuller, V.A. Schmidt, Hysteresis properties of titanomagnetites: Grain size and composition dependence, *Phys. Earth Planet. Inter.* 13 (1977) 260–266.
- [29] J.L. Kirschvink, The least-squares line and plane and the analysis of palaeomagnetic data, *Geophys. J. R. Astron. Soc.* 62 (1980) 699–718.
- [30] S.C. Cande, D.V. Kent, Revised calibration of the geomagnetic polarity timescale for the late Cretaceous and Cenozoic, *J. Geophys. Res.* 100 (1995) 6093–6095.
- [31] N.J. Shackleton, A. Berger, W.R. Peltier, An alternative astronomical calibration of the lower Pleistocene time-scale based on ODP Site 677, *Trans. R. Soc. Edinb. Earth Sci.* 81 (1990) 251–261.
- [32] B.S. Singer, M.S. Pringle, K.A. Hoffman, A. Chauvin, R.S. Coe, Dating transitionally magnetized lavas of the late Matuyama chron: toward a new $^{40}\text{Ar}/^{39}\text{Ar}$ timescale of reversals and events, *J. Geophys. Res.* 104 (1999) 679–693.
- [33] L. Tauxe, Sedimentary records of relative paleointensity of the geomagnetic field: theory and practice, *Rev. Geophys.* 31 (1993) 319–354.
- [34] J.W. King, S.K. Banerjee, J.A. Marvin, A new rock-magnetic approach to selecting sediments for geomagnetic paleointensity studies: application to paleointensity for the last 4000 years, *J. Geophys. Res.* 88 (1983) 5911–5921.
- [35] A.P. Roberts, B. Lehman, R.J. Weeks, K.L. Verosub, C. Laj, Relative paleointensity of the geomagnetic field over the last 200,000 years from ODP Sites 883 and 884, North Pacific Ocean, *Earth Planet. Sci. Lett.* 152 (1997) 11–23.
- [36] S. Brachfeld, S.K. Banerjee, A new high-resolution geomagnetic paleointensity record for the North American Holocene: a comparison of sedimentary and absolute intensity data, *J. Geophys. Res.* 181 (2000) 429–441.
- [37] T. Sato, H. Kikuchi, M. Nakashizuka, M. Okada, Quaternary geomagnetic field intensity: constant periodicity or variable period?, *Geophys. Res. Lett.* 25 (1998) 2221–2224.
- [38] R. Leonhardt, F. Heider, A. Hayashida, Relative geomagnetic field intensity across the Jaramillo subchron in sediments from the California margin: Ocean Drilling Program Leg 167, *J. Geophys. Res.* 104 (1999) 29133–29146.
- [39] C. Laj, C. Kissel, F. Garnier, E. Herrero-Bervera, Relative geomagnetic field intensity and reversals for the last 1.8 My from a central equatorial Pacific core, *Geophys. Res. Lett.* 23 (1996) 3393–3396.
- [40] K.L. Verosub, E. Herrero-Bervera, A.P. Roberts, Relative geomagnetic paleointensity across the Jaramillo subchron and the Matuyama/Brunhes boundary, *Geophys. Res. Lett.* 23 (1996) 467–470.
- [41] Y.S. Kok, L. Tauxe, A relative geomagnetic paleointensity stack from the Ontong-Java Plateau sediments for the Matuyama, *J. Geophys. Res.* 104 (1999) 25401–25413.
- [42] J. Imbrie, J.Z. Imbrie, Modeling the climatic response to orbital variations, *Science* 207 (1980) 943–953.